International Journal of Chemical, Materials and Biomolecular Sciences
ISSN: 2415-6620
Vol:7, No:1, 2013

Characterization of Biodegradable Nanocomposites with Poly (Lactic Acid) and Multi-Walled Carbon Nanotubes

Md F. Mina, Mohammad D.H. Beg, Muhammad R. Islam, Abu K. M. M. Alam A. Nizam, and Rosli M. Younus

***Abstract*—**In this study, structural, mechanical, thermal and electrical properties of poly (lactic acid) (PLA) nanocomposites with low-loaded (0−1.5 wt%) untreated, heat and nitric acid treated multi-walled carbon nanotubes (MWCNTs) were studied. Among the composites, untreated 0.5 wt % MWCNTs and acid-treated 1.0 wt% MWCNTs reinforced PLA show the tensile strength and modulus values higher than the others. These two samples along with pure PLA exhibit the stable orthorhombic α-form, whilst other samples reveal the less stable orthorhombic β-form, as demonstrated by X-ray diffraction study. Differential scanning calorimetry reveals the evolution of the mentioned different phases by controlled cooling and discloses an enhancement of PLA crystallization by nanotubes incorporation. Thermogravimetric analysis shows that the MWCNTs loaded sample degraded faster than PLA. Surface resistivity of the nanocomposites is found to be dropped drastically by a factor of 10^{13} with a low loading of MWCNTs (1.5 wt%).

***Keywords*—**Crystallization, multi-walled carbon nanotubes, nanocomposites, Poly (lactic acid).

I. Introduction

CARBON nanotubes (CNTs) reinforced polymeric nanocomposites have attracted considerable attention over pure polymers due to their enhanced thermal, mechanical and electrical performances [1–4]. These improvements in properties reportedly depends not only on the unique mechanical strength, high aspect ratio, excellent thermal and electrical conductivities of CNTs [5], but also on their alignment, adhesion and dispersion in polymer matrix as well as the degree of surface modification [6-8]. The formation of nanotubes agglomeration during mixing with polymer has been a major drawback of the development of CNT-based polymeric nanocomposites. Therefore, various ways have been employed to homogeneously disperse the nanotubes into the matrix [9-12]. Although, most of the previous research works on CNT-based composites were performed with synthetic plastics, bio-plastics have drawn a considerable interest to produce biodegradable nanocomposites recently [13-16]. Poly (lactic acid) (PLA) is a commonly used biodegradable polymer, which is being extensively studied for the purpose of replacing commodity polymers in near future. It consists of linear chain molecule, synthesized by ring opening polymerization or by condensation polymerization from the lactic acid monomers [17] and possesses good merits due to its melt processability, thermal and chemical resistance [18]. However, the brittleness and high-cost of PLA lose much of its potential in the fabrication of attractive materials for wide industrial applications.

In this study, PLA has been mixed well with untreated and treated multi-walled carbon nanotube (MWCNTs) of different compositions by extrusion in order to improve the dispersion of nanotubes, and then the ultimate nanocomposites were produced by injection molding. Besides, MWCNTs were subjected to both acid and heat treatments for their surface modification before incorporating into PLA. All the samples were characterized by X-ray diffraction (XRD) study, scanning electron microscopy (SEM), mechanical test, thermal measurements and electrical tests. Especially, the evolution of two different crystalline structures in PLA as induced by different types of MWCNTs under controlled cooling by differential scanning calorimetry (DSC) was an interesting finding, whereas the injection molded samples showed only one crystalline phase as studied by XRD. All these results were correlated with the observed mechanical and electrical properties of the samples and discussed in detail in the present study.

II. Experimental

A. Materials

PLA thermoplastic used in this study was collected from Nature Works® PLA, 2002D, USA, having the melt index of 5-7 g/10 min at a temperature 210 °C and specific gravity of 1.24. MWCNTs of diameter ~110−170 nm, length ~5−9 μm and purity~90% and nitric acid (HNO_3) were purchased from Sigma, Aldrich, USA.

B. Acid and Heat Treatments of MWCNTS

For acid treatment of MWCNTs, about 10 g of MWCNTs were dipped in 1000 mL of HNO_3 (2M) solution. A continuous stirring with heating at 80°C of the solution for 4 hours was performed. After this treatment, the MWCNTs

Md F. Mina is with the Faculty of Chemical and Natural Resources Engineering, Universiti Malaysia Pahang, Lebuhraya Tun Razak, Gambang-26300, Pahang, Malaysia; (e-mail: minamd.forhad@yahoo.com).
Mohammad D. H. Beg is with the Faculty of Chemical and Natural Resources Engineering, Universiti Malaysia Pahang, Lebuhraya Tun Razak, Gambang-26300, Pahang, Malaysia; (e-mail: dhbeg@yahoo.com).
Muhammad R. Islam is with the Faculty of Chemical and Natural Resources Engineering, Universiti Malaysia Pahang, Lebuhraya Tun Razak, Gambang-26300, Pahang, Malaysia; (e-mail: remanraju@yahoo.com).
Abu K. M. M. Alam is with the Faculty of Chemical and Natural Resources Engineering, Universiti Malaysia Pahang, Lebuhraya Tun Razak, Gambang-26300, Pahang, Malaysia; (e-mail: akmmalam@gmail.com).
A Nizam is with the Faculty of Chemical and Natural Resources Engineering, Universiti Malaysia Pahang, Lebuhraya Tun Razak, Gambang-26300, Pahang, Malaysia.
Rosli M. Yousuf is with the Faculty of Chemical and Natural Resources Engineering, Universiti Malaysia Pahang, Lebuhraya Tun Razak, Gambang-26300, Pahang, Malaysia.

containing solution was cooled down to room temperature and repeatedly diluted to reach the ultimate pH of 7 and filtered by 0.22 μm Millipore polycarbonate membranes using a vacuum pump. Heat treatment process of the original MWCNTs was done by heating them in a furnace up to 500°C and then cooled to room temperature.

C. Preparation of Composites

During composites fabrication, 0.05, 1.0, and 1.5 wt% MWCNTs contents were compounded with PLA by a twin screw extruder (Thermo Scientific Prism Eurolab-16, Germany) in the temperature profile ranging 110−190 °C with the screw rotating speed of 100-110 rpm. The extrudates were pelletized by chopper machine. Tests samples (Fig.1a) were prepared by a BOY15-S (Germany) injection molding machine in a temperature profile ranging 165-150°C with the screw rotating speed of 100-110 rpm 155 rpm. The highest values of mechanical properties as examined by the tensile test were considered as the optimized filler and further composites with acid and heat treated nanotubes were prepared by the optimum filler content.

D. Tensile Testing of Composites

Tensile testing was conducted according to ASTM 638-08, using a Shimadzu (Model: AG-1) Universal tensile machine fitted with a 5 kN load cell operated at a cross-head speed of 10 mm/min. Five samples of each category were tested for tensile strength (*TS*) and tensile modulus (*TM*) measurements, keeping a 65 mm gauge length.

E. Scanning Electron Microscopy

Fractured surface morphologies of nanocomposites were monitored by a scanning electron microscope (SEM) (model-ZEISS, EVO 50, Germany). For measurements, samples were placed onto a metal based holder with the help of double sided sticky carbon tape. Prior to observations, samples were coated with gold for composites by means of a vacuum sputter-coater for ease of conduction.

F. X-ray Diffraction Measurement

X-ray diffraction (XRD) measurements were conducted on tensile specimen of composites using a Rigaku MIniflex II, Japan (at 30 kV, 15 mA), which was equipped with a computer controlled software to set up the apparatus and analyze the data. For XRD studies, the samples were cut into a size of 2 cm×2 cm. The specimens were step-wise scanned over the scattering angle (2θ) from 5 to 40°, with a step of 0.02°, using CuK_α radiation of wavelength λ=1.541 Å. The data were collected in terms of the diffracted X-ray intensity (*I*) versus 2θ.

G. Thermogravimetric Analysis

Thermogravimetric measurements were performed by a thermogravimetric analyzer (TGA) (Q500 V6.4, Germany) in a platinum crucible under nitrogen atmosphere (flow rate 60 ml/min) with a heating rate of 20°C /min. The temperature range was scanned from 25 to 600° C.

H. Surface Resistivity Measurement

Surface resistivity (ρ_s) was measured at room temperature (28 °C) according to the set-up depicted in Fig. 1b by the direct current (DC) using the following formula [19]:

$$\rho_s = \left(\frac{U}{L} \times \frac{D}{I_s}\right) \quad (1)$$

where, U (volt) is the voltage drop across length L=0.01 (m) between two aluminium electrodes placed above the sample and I_s (ohm) is the surface current of the sample of width D=0.009 (m). Electrode size (length × width) was 0.018 m × 0.009 m. The DC voltage of 100 V was employed using a Keithely digital electrometer (Model 6517B, USA) and a micro-voltmeter, and the value of ρ_s was obtained in the unit of Ohm/m^2 as according to equation (1).

(i) (ii)

(a)

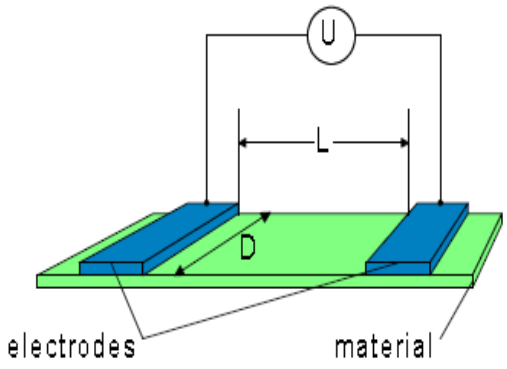

(b)

Fig. 1(a) Tensile specimen of (i) PLA and (ii) composites and (b) a schematic setup for resistivity measurement

III. Results and Discussions

A. Mechanical Properties

Fig. 2 illustrates the *TS* and *TM* values of PLA and its composites prepared with untreated and treated MWCNTs. Clearly, the *TS* and *TM* values of pure PLA and its nanocomposites are in proximity to each other. Nevertheless, a

slightly high *TS* and *TM* for pure PLA, 0.5PMWC, and APMWC compared to 1.0PMWC, 1.5PMWC and HPMWC is also observed. This increment in mechanical properties with very low loaded nanotubes and with their acid treatment are probably because of evolved crystalline structures of PLA and the interaction of its molecules with nanotubes. It was reported that acid treatment can functionalize MWCNTs with -COOH groups and increase surface roughness on the graphen layers, which can facilitate hydrogen bonding between fillers and PLA molecules [20]. In contrast, the lowering in TS and TM values can be attributed to poor dispersion of MWCNTs due to formation of small agglomeration, which was also reported in the literature for low loading of MWCNTs in polypropylene [21].

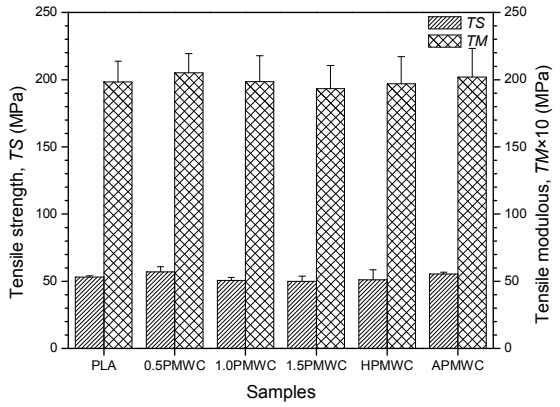

Fig. 2 *TS* and *TM* values of PLA and its composites prepared with untreated and treated MWCNTs

B. Structural Analysis

XRD profiles of injection molded (a) PLA, (b) 0.5PMWC, (c) 1.0PMWC, (d) 1.5PMWC, (e) HPMWC and (f) APMWC are shown in Fig.3. The important crystalline peak is diffused, appearing on a broad scattering, which is originated from the amorphous region of PLA. The broadly diffused peak suggests that PLA chains are poorly ordered with a low degree of crystallinity due to the rapid cooling of injection molded process. The peak position for PLA, 0.5PMWC and APMWC is observed close to 2θ ≈17.35°, while that for 1.0PMWC, 1.5PMWC and HPMWC appears at 2θ ≈16.3°, a lower angle compared to the previous one. To analyze these results, we introduce the reported crystalline structures of PLA, which shows the α-phase with pseudo-orthorhombic unit cell (*a* =10.7 Å, *b* =6.126 Å, and *c* =28.939 Å) and the *β*-phase with orthorhombic cell (*a* =10.31 Å, *b* =18.21 Å, and *c*= 9.0 Å), where the former one is more stable than the latter [22]. From these data, calculation shows that 200 reflection of the α-phase will appear at 2θ ≈17.28° and that of the *β*-phase at 2θ ≈16.56°. This analysis, therefore, dictates us to consider the appearance of α-crystal in pure PLA, 0.5PMWC and APMWC and *β*-crystal in 1.0PMWC, 1.5PMWC and HPMWC. Considering the diffuseness of peaks, the possibility of the presence of both phases in the samples cannot be ignored. However, the peak position indicates the most possible structures (α- and *β*-crystals) of PLA in the nanocomposites investigated here. As stated before that increasing MWCNTs content may facilitate the formation of agglomerates, which act as nucleating sites with high surface free energy for the less stable *β*-form of PLA. On the other hand, the formation of the stable α-phase was reported in organically-modified montmorillonite reinforced PLA [23], where the reinforcements were claimed to be homogeneously dispersed, acting as favorable nucleating agents for this phase. In our case, both α- and β- phases are developed in PLA, depending on nanotubes concentration and treatments, thereby governing the observed variations in mechanical properties of the samples.

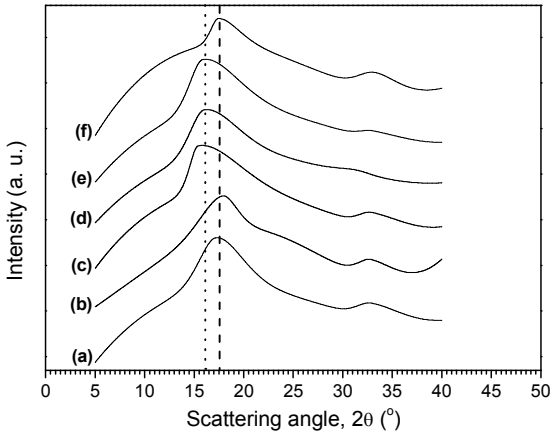

Fig. 3 XRD profiles of injection molded (a) PLA, (b) 0.5PMWC, (c) 1.0PMWC, (d) 1.5PMWC, (e) HPMWC and (f) APMWC

C. Thermal Properties

Fig. 4i illustrates the DSC thermograms obtained at first heating of the injection molded samples. In the DSC curves, one can notice the variations in glass transition temperature (T_g) at 58−67 °C, cold crystallization temperature (T_c) at 80−105 °C and melting temperature (T_m) at 150−170 °C, depending on the processing conditions (filler content and treatment) of samples. Although the T_g and T_m values are observed to be nearly the same for all samples, the heat capacity (ΔC_p) during glass transition and the pattern of glass transition peak of 1.0PMWC, 1.5PMWC and HPMWC shows a significantly different look from that of PLA, 0.5PMWC and APMWC. This variation in glass transition can be attributed to the difference in molecular mobility that is responsible for the difference in crystalline structures (α- and *β*- phases) of the samples. Most often, it is a common trend to show a high T_g by a sample with a high degree of crystallinity, because the non-crystalline molecular chains are anchored to the more orderly crystalline states and are less mobile. The high values of ΔC_p may represent the cooperative molecular movement of PLA during transition from its glassy state to toughened state. It can be assumed that the high agglomeration of MWCNT facilitate a large number of PLA macromolecules at its periphery to readily and cooperatively move during the glass transition. Compared with PLA, the T_c of nanocomposites

occurs at lower temperatures, indicating an early crystallization of PLA after MWCNTs incorporation. In other words, nanotubes and their increasing amounts sufficiently induce the crystallization in PLA. As the nanotubes content increases, available surface area for heterogeneous nucleation in PLA also increases, thereby decreasing the T_c value. On the other hand, single melting peak is observed for each sample with a shoulder at the onset, which varies from sample to sample. Obviously, the T_m peak position also varies, based on the samples.

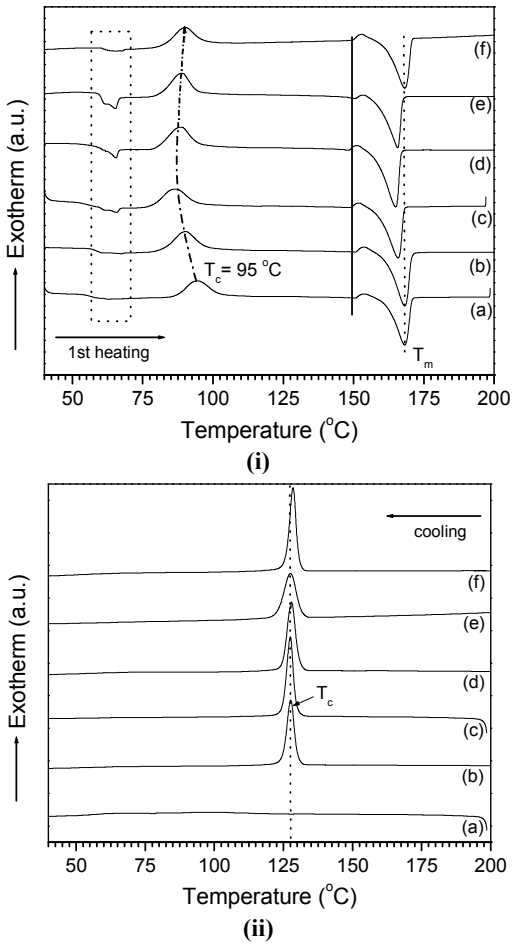

Fig. 4 DSC thermograms obtained at first heating (i) and cooling (ii) cycles of the samples

Fig. 4ii displays the DSC curves on cooling of the samples after first heating. The most striking finding here is that pure PLA remains amorphous under cooling as it does not show any recrystallization peak, whereas all nanocomposites recrystallize at $T_c \approx 125$ °C. The strong T_c peak clarifies that MWCNTs act as an effective nucleating agent on the crystallization of PLA by cooling from the its melt. Besides, a careful observation points out that this recrystallization commences sooner in HPMWC than any other sample, most likely because of interaction between functionalized nanotubes and PLA molecules. In the 2nd heating runs (Fig. 5), pure PLA clearly exhibits the T_g, T_c and T_m peaks with a shoulder at T_m, whilst nanocomposites do not show any glass transition and crystallization but reveals double melting behavior with no observable concurrent shoulder. These results demonstrate that pure PLA is not crystallized during cooling but crystalizes from its amorphous state on 2nd heating, while all nanocomposites were completely crystallized during cooling due the presence of fillers. The double melting characteristics might be related to the two different crystalline structures developed in composites during controlled cooling process in the DSC cell [24], not found for the injection molded samples. The amount of enthalpies is an indicator of the crystal population for these two phases. Evidently, one of the double melting peaks occurs at 163-165 °C and the other one at 167-169 °C, which, according to analysis, indicates the α-phase. Therefore, 2nd heating results in α-phase for pure PLA and both phases for nanocomposites in which the population of β-phase is large. The population ratio of two phases (α: β) from melting enthalpies is analyzed to be 1:50. Due to separate crystalline structures, the stacked lamellar morphology of these two populations of PLA crystallites may be differed in lamellar thicknesses. Reportedly, the melting temperature of lamellar crystals is related to the following equation [21]:

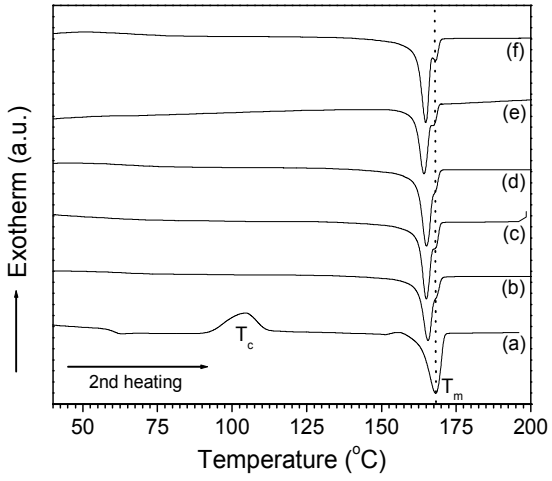

Fig. 5 DSC thermograms obtained at second heating cycle of the samples

where T_m is the observed melting point for the lamella of thickness l_c, σ_e is the surface free energy, ΔH_m^0 is the enthalpy of fusion for 100% crystalline PLA and T_m^0 is the melting temperature of infinitely large crystal. If T_m^o, σe and ΔH_m^0 are assumed as constants, the T_m will change if l_c changes that help explain the double melting points of composites. In this context, an interaction between MWCNTs with the PLA matrix is notable, because the nanotubes surface act as suitable nucleation sites to promote the growth and formation of transcrystalline regions for organizing different lamellae in PLA, as was suggested elsewhere [25]. During

melt annealing process in DSC, MWCNTs may provide confined space and the low surface energies for rearrangement of PLA chains and thin lamellar crystal could be generated.

Fig. 6 demonstrates the TGA thermograms, where the start of weight-loss for various samples is indicated by an arrow. The weight-loss patterns for the samples are almost the same except the start of weight-fall, which depends on MWCNTs loading. Apparently, the onset of decomposition occurs earlier in APMWC than in any other sample. This difference in onset temperature can be explained by the following way, as reported elsewhere [21]. The high thermal conductivity of nanotubes may create localized high temperature in MWCNTs lumps as compared to PLA matrix for which the PLA molecules at the periphery of the lumps may start to degrade earlier. Besides, functionalized MWCNTs by nitric acid treatment can form the hydrogen bonding with PLA, which can ease the thermal conduction in APMWC and causes its early degradation. The degradation temperature (T_d) obtained from the differential TG curves of PLA, 0.5PMWC, 1.0PMWC, 1.5PMWC, HPMWC and APMWC are 345, 338, 332, 331, 333, and 332 °C, respectively.

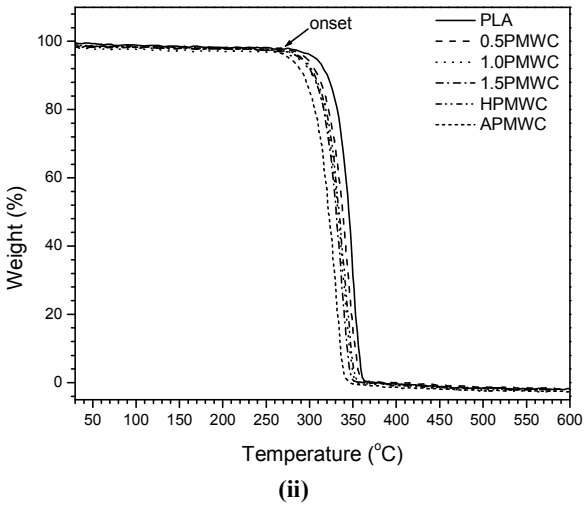

Fig. 6 TGA thermograms of the samples

D.Surface Morphology

The SEM micrographs of the fractured surfaces of (a) PLA, (b) 1.0PMWC and (c) APMWC are presented in Fig.7. Surface of PLA shows some striations and seems to be comparatively clean. On the other hand, a number of chunks are found on the surface of 1.0PMWC that may indicate the PLA crystallites. In contrast, huge numbers of small chunks are observable on the surface of APMWC. Apparently, the number of crystallites is large in nanocomposites. Cracks and striations develop in nanocomposites more than pure PLA after fracture.

E. Surface Resistivity

The surface resistivity, ρ_s, for different samples are shown in Fig.8, where a high ρ_s value indicates a less conductivity in the sample. The pure PLA exhibits the highest value of ρ_s =1.13×10^{15} ohm/m^2 and 1.5PMWC shows the lowest value of ρ_s =1.14×10^{2} ohm/m^{2,} indicating a significant decrease in resistivity by a factor of 10^{13}. Thus, it testifies that a slight addition of MWCNTs content in PLA makes a drastic fall of surface resistance, which is similar to those published elsewhere [21, 26]. These authors claimed that CNT has a high aspect ratio and many π-bonds (C=C bond), which drive electrons easily in the nanocomposites.

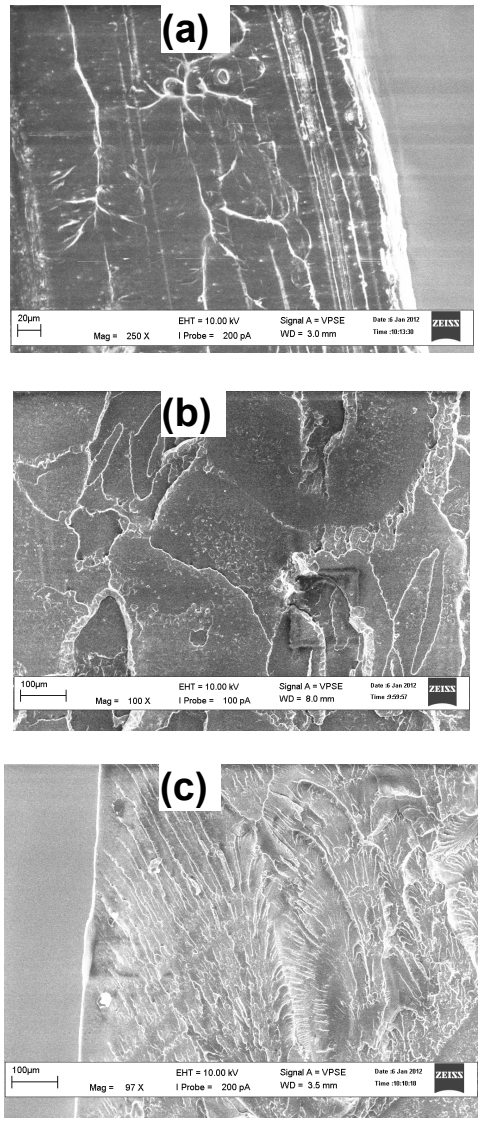

Fig. 7 SEM micrographs of the fractured surfaces of (a) PLA, (b) 1.0PMWC and (c) APMWC

This remarkable improvement in surface conductivity in the nanocomposites by addition of CNT suggests a good dispersion of MWCNTs, where the high nanotubes content and their heat treatment provide superior electrical conductivity.

IV. Conclusion

Inclusion of MWCNTs enhances the mechanical and electrical properties of the PLA nanocomposites, suggesting a good dispersion of nanotubes by extrusion followed by injection molding. While the lower content of MWCNTs gives rise to the stable α-crystal in PLA, the higher content favors the formation of the less stable β-crystal in PLA. Heat treatment of nanotubes results in β-phase but acid treatment gives rise to α--phase.

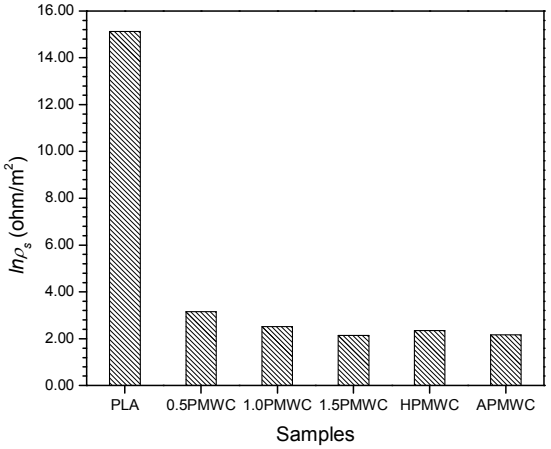

Fig. 8 Surface resistivity of different samples

A complete crystallization in PLA by MWCNTs reinforcement is observed by DSC during cooling, while pure PLA remains amorphous state. MWCNTs induce crystallization of both phases under controlled cooling in the DSC cell, where the crystal population of β-phase is larger than that of α-phase. Thermal degradation temperature decreases in the samples with the increase of nanotubes as a result of the increased thermal conductivity in the nanocomposites due to the presence of MWCNTs. Decreased surface resistivity by incorporation of MWCNTs makes the PLA nanocomposites more conductive.

Acknowledgment

The authors like to thanks Ministry of Higher Education Malaysia to support for this project through FRGS 100114.

References

[1] S. J. Park, M. S. Cho, S. T. Lim, H. J. Choi and M. S. Jhon. Synthesis and dispersion characteristics of multi-walled carbon nanotube composites with poly (methyl methacrylate) prepared by in-situ bulk polymerization. Macromol Rapid Commun 24:1070–1073, 2003.

[2] N. Grossiord, J. Loos, O. Regev and C. E. Koning. Toolbox for dispersing carbon nanotubes into polymers to get conductive nanocomposites. Chem Mater 18:1089–1099, 2006.

[3] R. Andrews and M. C. Weisenberger. Carbon nanotube polymer composites. Curr Opin Solid State Mater Sci 8:31–37, 2004.

[4] Y. T. Sung, M. S. Han, K. H. Song, J. W. Jung, H. S. Lee, C. K. Kum, J. Joo and W. N. Kim. Rheological and electrical properties of polycarbonate/multi-walled carbon nanotube composites. Polymer 47:4434– 4439, 2006.

[5] A. Maity and M . Biswas. Recent progress in conducting polymer, mixed polymer-inorganic hybrid nanocomposites. J Ind Eng Chem 12:311–351, 2006.

[6] N. Grossiord, J. Loos, C. E. Koning. Strategies for dispersing carbon nanotubes in highly viscous polymers. J Mater Chem 15:2349–2352, 2005.

[7] S. S. Ray, S. Vaudreuil, A. Maazouz and M. Bousmina. Dispersion of multi-walled carbon nanotubes in biodegradable poly (butylene succinate) matrix. J Nanosci Nanotech 6:2191–2195, 2006.

[8] S. Vaudreuil, A. Labzour, S. S. Ray, K. E. Mabrouk and M. Bousmina. Dispersion characteristics and properties of poly (methyl methacrylate)/multi-walled carbon nanotubes nanocomposites. J Nanosci Nanotech 7:2349–2355, 2007.

[9] S. T. Kim, H. J. Choi and S. M. Hong. Bulk polymerized polystyrene in the presence of multiwalledcarbon nanotubes. Colloid Polym Sci 285:593–598, 2007.

[10] H. J. Lee, S. J. Oh, J. Y. Choi, J. W. Kim, J. W. Han, L. S. Tan and J. B. Baek. In situ synthesis of poly(ethylene terephthalate) (PET) in ethylene glycol containing terephthalic acid and functionalized multiwalled carbon nanotubes (MWNTs) as an approach to MWNT/PET nanocomposites. Chem Mater 17:5057–5064, 2005.

[11] R. Andrews, D. Jacques, D. Qian and T. Rantell. Multiwall carbon nanotubes: synthesis and application. Acc Chem Res 35:1088–1017, 2002.

[12] M. Moniruzzaman and K. Winey. Polymer nanocomposites containing carbon nanotubes. Macromolecules 39:5194–5205, 2006.

[13] Chin-San Wu, Hsin-Tzu Liao, Study on the preparation and characterization of biodegradable polylactide/multi-walled carbon nanotubes nanocomposites, Polymer 48, 4449–4458, 2007.

[14] B. Kumar, M. Castro and J.F. Feller. Poly (lactic acid)–multi-wall carbon nanotube conductive biopolymer nanocomposite vapour sensors, Sensors and Actuators B 16, 621– 628, 2012.

[15] S. W. Ko, M. K. Hong, B. J. Park, R. K. Gupta, H. J. Choi, S. N. Bhattacharya, Morphological and rheological characterization of multi-walled carbon nanotube/PLA/PBAT blend nanocomposites, Polym. Bull. 63:125–134, 2009.

[16] Chen-Feng Kuana, Chia-Hsun Chena,_, Hsu-Chiang Kuana, Kun-Chang Lina, Chin-Lung Chiangb, Hsin-Chin Penga Multi-walled carbon nanotube reinforced poly (L-lactic acid) nanocomposites enhanced by water-crosslinking reaction, Journal of Physics and Chemistry of Solids 69, 1399–1402, 2008.

[17] A. Bhatia, R. K. Gupta, S. N. Bhattacharya, H. J. Choi. Compatibility of biodegradable poly (lactic acid) (PLA) and poly (butylene succinate) (PBS) blends for packaging application. Korea-Australia Rheol J 19:125–131, 2007.

[18] T. M. Wu and M. F. Chiang. Fabrication and characterization of biodegradable poly (lactic acid)/ layered silicate nanocomposites. Polym Eng Sci 45:1615–1621, 2005.

[19] Michael B. Heaney. The Measurement, Instrumentation and Sensors Handbook, chapter Electrical Conductivity and Resistivity. CRC Press, 1999.

[20] Chin-San Wu, Hsin-Tzu Liao, Study on the preparation and characterization of biodegradable polylactide/multi-walled carbon nanotubes nanocomposites. Polymer 48 4449-4458, 2007.

[21] M. A. Haque, M. F. Mina, A.K.M. M. Alam, M. J. Rahman, M. A. H. Bhuiyan, and T. Asano, Multi-Walled Carbon Nanotubes Reinforced Isotactic Polypropylene Nanocomposites: Enhancement of Crystallization and Mechanical, Thermal and Electrical Properties, *Polymer Composites*, 33, 1094-1104, 2012.

[22] W, Hoogsteen, A. R. Postema, Pennings AJ, Brinke GT. Crystal Structure, Conformation, and Morphology of Solution-Spun Poly(L-lactide) Fibers Macromolecules 1990; 23: 634–642.

[23] T. M. Wu, C. Y. Wu. Biodegradable poly(lactic acid)/chitosan-modified montmorillonite nanocomposites: Preparation and characterization. Polym Degrad Stab; 91: 2198-2204, 2006.

[24] M. Pluta and A. Galeski. Crystalline and supermolecular structure of polylactide in relation to the crystallization method. J Appl Polym Sci; 86: 1386, 2002.

[25] P. V. Joseph, K. Joseph, C. K. S. Thomas Pillai, V. S. Prasad, G. Groeninckx and M. Sarkissova. The thermal and crystallization studies of short sisal fiber reinforced polypropylene composite. Composite Part A, 34(3), 253-266, 2003.

[26] Chen-Feng Kuana, Hsu-Chiang Kuana, Chen-Chi M. Mab, Chia-Hsun Chena Mechanical and electrical properties of multi-wall carbon nanotube/poly(lactic acid) composites, Journal of Physics and Chemistry of Solids 69, 1395–1398, 2008.